The kinkiness of cumulenones: H_2C_3O, H_2C_4O, and H_2C_5O

Allan L. L. East
Steacie Institute for Molecular Sciences, National Research Council, Ottawa, Ontario K1A 0R6, Canada

(Received 29 September 1997; accepted 11 November 1997)

The floppiest bending or ''kinking'' modes of propadienone (H_2CCCO), butatrienone (H_2CCCCO), and pentatetrenone ($H_2CCCCCO$) are investigated with high-quality *ab initio* methods. The potential surface for bending at the β-carbon atoms of these species is very flat for the C_4 and C_5 species, and together with zero-point energy contributions from the other vibrations, it is concluded that the barriers to linearity of their carbon chains are less than 1 kJ mol^{-1}, if they exist at all. Comparisons are made to published experimental values for rotational constants and floppy-mode barrier heights (from gas-phase microwave spectra) and vibrational fundamentals (from matrix infrared spectra). Consensus is achieved for propadienone and butatrienone, and the arguments for infrared detection of synthesized pentatetrenone in an argon matrix are strongly supported by our calculations. [S0021-9606(98)00707-7]

I. INTRODUCTION

Nonrigid or ''floppy'' molecules are those which possess one or more facile vibrational motions, each characterized by a very flat one-dimensional curve on the potential surface for nuclear motions. Determination of equilibrium molecular structures in these cases is more challenging than for rigid molecules. One of the most accurate experimental techniques in these cases is the fitting, to spectroscopically determined rovibrational energy levels, of a semirigid bender Hamiltonian[1] possessing geometrical parameters. This Hamiltonian has seen many implementations[2–18] in the determination of molecular geometries and shapes of flat potential curves. For small molecules (up to four or five atoms), results have demonstrated erroneous predictions of certain (low) levels of *ab initio* theory in cases where the flat potential surfaces have features on the order of 50 cm^{-1} or less. For larger molecules, however, many more approximations must be made to keep the number of variables at a manageable size; typical uses of this model in these cases either allow only a subset of the molecular internal coordinates to relax upon bending the molecule along the mode of interest, or else incorporate *ab initio* structural information. Two notable floppy molecule examples of the interplay of the semirigid bender model and *ab initio* theory are fulminic acid (HCNO)[2,8,19–24] and carbon suboxide (OCCCO).[3,25–29]

The molecules of concern here are members of the cumulenone series H_2O_nO, which are candidates for astrophysical detection. The penchant for kinking in these molecules can be understood[30] with simple valence-bond Lewis-dot resonance representations of these systems, displayed in Fig. 1 for butatrienone. The principal resonance structure involves consecutive double bonds throughout the carbon chain, while the secondary one arises from donation of an oxygen lone pair to create a triple bond to the α-carbon (C_α) and a lone pair on the β-carbon (C_β). An extended resonance structure exists in which a second triple bond is formed, with a lone pair appearing on the δ-carbon (C_δ). Significant contribution of the second resonance structure will flatten the $\theta_{\alpha\beta\gamma}$ bending potential, and the question of whether or not the contribution is strong enough in H_2C_4O and H_2C_5O to cause kinked equilibrium and ground-state structures has not yet been resolved. We refer to $\theta_{\alpha\beta\gamma}$ (or simply θ_β) as the *principal* angle. At the equilibrium geometry and the ''effective'' (or ''averaged'') ground-state geometry, the principal angle will be denoted as θ_{eq} and θ_{eff}, respectively, with the corresponding barriers to chain linearity being V_{eq} and V_{eff}.

In initial spectroscopic work in the 1970's on propadienone,[31] R. D. Brown and co-workers at Monash University saw indications of non-C_{2v} symmetry which became concrete as their work continued.[32–35] Parallel *ab initio* work at the Hartree–Fock level showed only a C_{2v} potential minimum;[36,37] in 1982 the inclusion of low levels of electron correlation shifted the minimum to an in-plane bent C_s structure, with their best results giving values for θ_{eq} and V_{eq} of 145 deg and 370 cm^{-1}, respectively.[38] Brown and coworkers ultimately performed a semirigid bender analysis on propadienone,[11] published in 1987, resulting in $\theta_{eff}=142°$ and $V_{eff}=359$ cm^{-1} for the ground-state bending potential. It is of interest to update the outmoded *ab initio* prediction to see if the current level of agreement is maintained.

In 1986 a semirigid bender calculation by R. D. Brown and co-workers for H_2C_4O, using limited degrees of freedom, suggested a C_{2v} structure ($\theta_{eff}=180°$).[10] This is in contrast to the results of a 1984 *ab initio* study,[39] whose small-basis MP2 and MP3 energy calculations at various constrained geometries suggested that the equilibrium structure of H_2C_4O is kinked out-of-plane with a barrier to chain linearity of $V_{eq}>300$ cm^{-1}.

Experimental matrix-infrared (IR) spectra have been obtained for these molecules. Two matrix-IR spectra of propadienone (in Ar and N_2 hosts) were reported by Chapman, Miller, and Pitzenberger in 1987, without vibrational assignment.[40] R. F. C. Brown and co-workers reported several argon-matrix IR absorbances of butatrienone in 1990,[41] and of the more unstable pentatetrenone molecule in 1988.[42]

This work examines the kinking nature of cumulenones

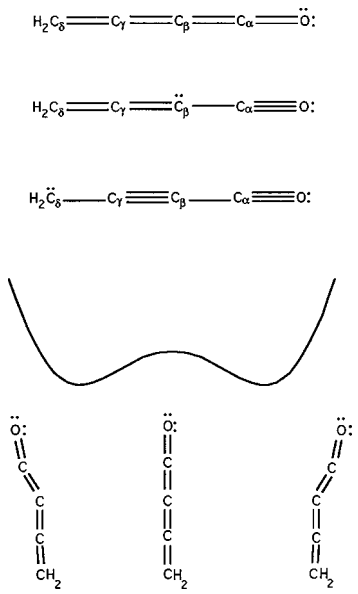

FIG. 1. Principal, secondary, and extended Lewis-dot resonance structures for the example of butatrienone (top half of figure), and a schematic of the floppy bending mode double-well potential (bottom half of figure).

in their singlet ground states with top-of-the-line levels of *ab initio* theory. Geometrical structures and barriers to chain linearity are examined, and rotational constants, dipole moments, and vibrational frequencies are also determined for comparison to experimental results.

II. THEORETICAL METHODS

Standard *ab initio* molecular orbital calculations[43] were performed at a number of levels of theory, using various versions of the GAUSSIAN[44] and MOLPRO[45] codes. Basis sets were taken from Pople and co-workers[46–49] or Dunning and co-workers.[50,51] Beyond the molecular orbital approximation of Hartree–Fock (HF) theory, the effect of electron correlation on internal rotation barriers was investigated using Møller–Plesset many-body perturbation theory (MP2, MP3, MP4, MP5)[52–55] and quadratic configuration interaction theory [QCISD, QCISD(T), QCISD(TQ)].[56–58] Coupled cluster theory [CCSD, CCSD(T)][59,60] was briefly examined but was found to give very similar results to QCI. In the case where MP5 was possible, extrapolation of the MP*n* series (MP∞) was performed with the shifted [1,2] Padé approximant.[61–64] The harmonic frequencies were evaluated via analytic MP2 second derivative techniques[65,66] using GAUSSIAN. Normal modes were assigned using total energy distribution (TED) analysis,[67–69] and infrared intensities were computed with the double-harmonic approximation,[70,71] both using the INTDER program.[72] Generally, in all electron-correlated calculations the 1*s* core electrons were frozen; the (fu) designation (full correlation) will designate the exceptions.

III. BARRIERS TO CHAIN LINEARITY

First, 36 pairs of fully optimized linear (C_{2v}) and kinked (C_s) structures of propadienone (17 pairs), butatrienone (11), and pentatetrenone (8) were obtained, employing various basis sets and levels of electron correlation. In 35 of the 36 cases, the C_s stationary point is the minimum and the C_{2v} stationary point is the transition state for interconversion between equivalent C_s minima; in the lone exception, the C_s optimization collapsed to the C_{2v} minimum. All of our optimized C_s equilibrium structures have the bond angle at C_β bent the most, with this kink forcing slight kinks in the rest of the heavy-atom chain, in an all-*trans* or zigzag fashion. The direction of the kink is out-of-plane for *n* even and in-plane for *n* odd, as forecast in earlier work;[39] this is obviously forced by the symmetry of the donating lone pair on oxygen, which is out-of-plane for *n* even and in-plane for *n* odd.

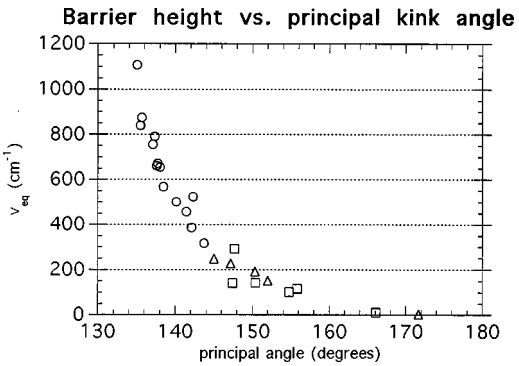

FIG. 2. Plot of barriers to chain linearity (V_{eq}) versus principal kink angle ($\theta_{eq}=\theta_\beta=\theta_{C_\alpha C_\beta C_\gamma}$) obtained at various levels of *ab initio* theory for H_2C_3O (circles), H_2C_4O (squares), and H_2C_5O (triangles).

Quite varied predictions were obtained for V_{eq} and θ_{eq}, and a strong correlation between the two was observed. The plot of V_{eq} versus θ_{eq}, using all of the electron-correlated optimization results (no HF ones), is presented in Fig. 2. Each point on the plot represents a two-parameter double-well potential for the floppy mode (the barrier height and location of the minimum being two suitable parameters), and the plot suggests that changing the level of *ab initio* theory is only affecting one degree of freedom in the double-well potential.

Since V_{eq} can be more easily estimated at higher levels of theory than θ_{eq}, more precise determinations of the barriers to chain linearity for all three cumulenones were carried out, with single-point energy computations using consistently the C_s and C_{2v} optimized geometries produced by QCISD/6-31G(*d*). The resulting barrier heights $V_{eq}=E(C_{2v})-E(C_s)$ are plotted against level of electron correlation theory employed in the calculations, and shown in Figs. 3–5.

For H_2C_3O (Fig. 3), and to a reasonable extent the longer compounds (Figs. 4 and 5), the correlation profiles past MP2 are very similar regardless of basis set. Even the inferior 6-31G basis set has a similar profile (Fig. 3), although the agreement is not as quantitative and does not begin until past MP3. A second general feature of the correlation profiles is that the MP3 barriers tend to be closer to QCISD ones rather than QCISD(T) ones for propadienone, but the opposite is true for H_2C_4O and H_2C_5O.

The basis set effects are very significant. The trend with the Dunning series cc-pVDZ/cc-VDZ, aug-cc-pVDZ, cc-

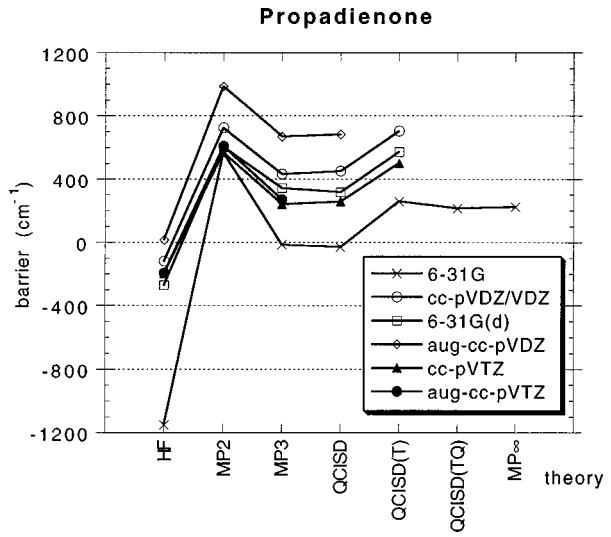

FIG. 3. Correlation profiles for the barrier to chain linearity (V_{eq}) of H_2C_3O using six different basis sets. Barrier is computed as $E(C_{2v})-E(C_s)$ using optimized QCISD/6-31G(d) geometrical structures. Level of correlation improves from left to right. The best basis sets (cc-pVTZ and aug-cc-pVTZ) are represented with filled-in symbols for easier visualization. The designation cc-pVDZ/VDZ indicates that hydrogen p-functions were removed from the traditional cc-pVDZ basis set.

pVTZ, aug-cc-pVTZ is toward structures less kinked than those actually obtained. The Pople basis sets were of limited use due to linear dependence problems when the diffuse functions were applied to the linear cumulenone chains.[73] The problem prevents their normal use for butatrienone and pentatetrenone, but could be circumvented without function deletion for propadienone. For this molecule, the 6-311 $+G(2df,p)$ basis set gave considerably smaller barriers at each level of correlation than the supposedly equivalent Dunning bases, cc-pVTZ and aug-cc-pVTZ. With an earlier indication that this basis set is less accurate (on this fine scale) than the aug-cc-pVTZ basis,[74] together with its linear dependence problems in the present case, we dismiss its results from further consideration.

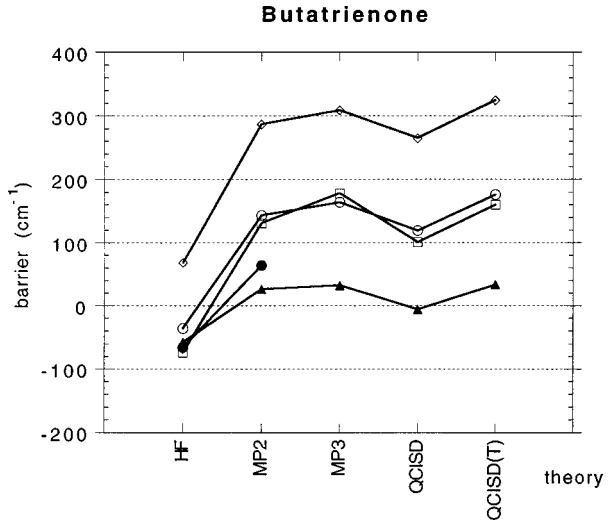

FIG. 4. Correlation profiles for the barrier to chain linearity (V_{eq}) of H_2C_4O using five different basis sets. See Fig. 3 for notes and basis set legend.

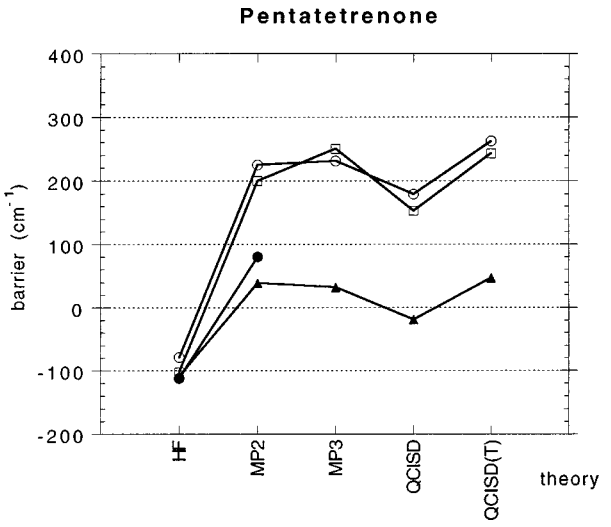

FIG. 5. Correlation profiles for the barrier to chain linearity (V_{eq}) of H_2C_5O using five different basis sets. See Fig. 3 for notes and basis set legend.

We shall take the best barrier heights from these figures [the QCISD(T)/cc-pVTZ//QCISD/6-31G(d) ones] and examine remaining corrections.

A. Valence correlation beyond QCISD(T)

The (T) corrections of $\sim+250\ \mathrm{cm}^{-1}$ for propadienone prompted an investigation of better correlation methods. Only the 6-31G basis set was small enough to allow us to compute propadienone barriers with more complete valence electron correlation (Fig. 3). Although the Møller–Plesset series convergence is poor (barriers in cm^{-1} for MP2, MP3, MP4, MP5: 568, -14, 500, 45), the QCISD(TQ) and MP∞ values (213 and $224\ \mathrm{cm}^{-1}$) lend strong support to the QCISD(T) value ($258\ \mathrm{cm}^{-1}$) as a good estimate of the correlation limit [full configuration interaction (CI)] value, suggesting only a modest decrease of $-1/7$ the effect of the (T) correction ($40\ \mathrm{cm}^{-1}$ for 6-31G). We expect this $-$(T)/7 effect for H_2C_3O to be similar for the better basis sets as well, due to the similar correlation profiles, and hence apply a correction of $-35\ \mathrm{cm}^{-1}$ for propadienone. The $-$(T)/7 correction is approximately $-5\ \mathrm{cm}^{-1}$ for H_2C_4O and H_2C_5O.

B. Geometry improvements

The largest deficiency of the QCISD/6-31G(d) geometries in computing the floppy-mode barrier height would be

TABLE I. Barriers to chain linearity [$V_{eq}=E(C_{2v})-E(C_s)$, cm^{-1}] with the cc-pVTZ basis set, using two different sets of C_s and C_{2v} geometries.

Molecule	H_2C_3O		H_2C_4O		H_2C_5O	
Geometry set[a]	A	B	A	B	A	B
HF	-197	-178	-58	5	-109	-18
MP2	569	596	26	24	39	12
MP3	240	232	32	26	32	6
QCISD	257	255	-6	13	-19	0
QCISD(T)	502	499	33	23	47	10

[a]Set A: QCISD/6-31G(d). Set B: MP2(fu)/cc-pVTZ.

TABLE II. Minimum-energy (kinked, C_s symmetry) structures for H_2C_3O.[a,b]

Basis set	Method	r_{CH}^{trans}	r_{CH}^{cis}	$r_{\beta\gamma}$	$r_{\alpha\beta}$	r_{CO}	θ_{HCH}	θ_{HCC}^{trans}	θ_{HCC}^{cis}	θ_β	θ_α
6-31G(d)	HF	1.0784	1.0784	1.3043	1.2685	1.1557	116.03	121.98	121.98	180.00	180.00
6-31G(d)	MP2	1.0885	1.0909	1.3397	1.3208	1.1849	115.54	120.80	123.66	137.69	166.47
cc-pVDZ	MP2	1.0980	1.1004	1.3506	1.3359	1.1790	116.12	120.37	123.51	135.47	166.73
6-311G(d,p)	MP2	1.0885	1.0911	1.3401	1.3200	1.1720	116.07	120.59	123.35	137.62	167.84
aug-cc-pVDZ	MP2	1.0955	1.0980	1.3536	1.3373	1.1825	116.54	120.35	123.10	135.04	166.48
cc-pVTZ	MP2(fu)	1.0797	1.0818	1.3265	1.3021	1.1701	116.39	120.86	122.75	142.29	169.01
6-31G(d)	MP2(fu)	1.0882	1.0906	1.3376	1.3174	1.1839	115.52	120.89	123.59	138.47	166.97
6-31G(d)	MP4	1.0920	1.0943	1.3462	1.3295	1.1953	115.70	120.62	123.69	137.36	164.79
6-31G(d)	QCISD	1.0902	1.0920	1.3341	1.3148	1.1814	115.84	120.94	123.22	143.71	166.63
6-31G(d)	QCISD(T)(fu)	1.0913	1.0932	1.3419	1.3221	1.1843	115.82	120.75	123.43	140.14	165.59
Prediction:		1.08(1)	1.08(1)	1.33(1)	1.31(1)	1.17(1)	116.5(5)	120.8(5)	123.0(5)	142(3)	167(2)
SRB[c]		1.094		1.313	1.295	1.168	122.4	116.9	120.7	142.0	164.5
Integrated SRB[d]		1.094(2)		1.322(1)	1.331(6)	1.162(2)	121.8(3)	117.2(1)	121.0(2)	143.5(1.0)	164.9(3.0)
r_s[e]		1.094(2)		1.322(1)	1.320(8)	1.163(2)	121.8(3)	117.2(1)	121.0(2)	144.5(1.5)	169.4(3.5)

[a]Bond lengths r in Å, bond angles θ in degrees. α,β, etc., denote carbon atoms counting from the oxygen end of the molecule.
[b](fu) means all electrons correlated; otherwise, the core electrons are frozen in the correlation treatments.
[c]Table VI of Ref. 11.
[d]Table XI of Ref. 11.
[e]Reference 35.

in the distance from the minimum to the saddle point along the floppy mode (θ_β). The QCISD/6-31G(d) values for θ_{eq} for H_2C_3O, H_2C_4O, and H_2C_5O are 143.7, 154.8, and 152.0°, respectively. However, recalling the hand-in-hand correspondence between *ab initio* V_{eq} and θ_{eq} values (Fig. 2), our best barrier heights from Figs. 3–5 of roughly 500, 40, and 80 cm^{-1}, respectively, suggest that the corresponding θ_{eq} values might be nearer to 140, 160, and 156°, respectively. The MP2(fu)/cc-pVTZ level of theory produced barrier predictions of ~550, 25, and 50 cm^{-1} for the three molecules in Figs. 3–5, and hence the fully optimized MP2(fu)/cc-pVTZ geometries should produce more realistic values for θ_{eq} for all three cumulenones. At any rate, the second set of geometries offers different degrees of kinkiness, and computed barriers with these can provide a measure of how sensitive the high-level V_{eq} values are to geometry differences. Table I compares barrier heights computed with the cc-pVTZ basis set using both sets of geometries. The effect is larger in the cases where the two C_s structures disagree more on the amount of kink; the difference in θ_{eq} values (θ_{eq}[MP2(fu)/cc-pVTZ]$-\theta_{eq}$[QCISD/6-31G(d)]) is 2 for H_2C_3O, 11 for H_2C_4O, and 20° for H_2C_5O. We estimate the improvements to our current best V_{eq} values due to better geometry selection to be 0 for H_2C_3O, -7 for H_2C_4O, and -25 cm^{-1} for H_2C_5O.

C. Basis set and core correlation

In an accurate determination of the barrier height in the double-well inversion mode of ammonia,[75] corrections for core ($1s$) correlation, relativity, and Born–Oppenheimer effects were determined to be (in cm^{-1}) -67, $+24$, and -11. We ignore the two smaller effects, and examine the correction for core correlation together with further basis set improvements, as we found them interdependent. At the MP2 level of theory and now using MP2(fu)/cc-pVTZ geometries, we computed barriers with the PZ($3d2f,2p1d$) basis set, with and without the core electrons active in the correlated calculation. This basis set was thought to provide 30 cm^{-1} accuracy in the case of the inversion barrier of ammonia,[74] although this has recently come into question,[76] and the effects of larger basis sets for these cumulenones are already under investigation.[77] Here the net effects [namely,

TABLE III. Minimum-energy (kinked, C_s symmetry) structures for H_2C_4O.[a,b]

Basis set	Method	r_{CH}	$r_{\gamma\delta}$	$r_{\beta\gamma}$	$r_{\alpha\beta}$	r_{CO}	θ_{HCH}	θ_γ	θ_β	θ_α	τ_{HCCC}[c]
6-31G(d)	HF	1.0744	1.2981	1.2702	1.2748	1.1471	118.91	179.18	167.99	176.85	90.14
6-31G(d)	MP2	1.0853	1.3181	1.2908	1.3025	1.1836	118.28	176.69	150.36	171.86	90.71
cc-pVDZ	MP2	1.0940	1.3288	1.3016	1.3166	1.1777	119.49	176.49	147.41	171.61	90.71
6-311G(d,p)	MP2	1.0846	1.3199	1.2848	1.2965	1.1716	119.38	177.16	155.86	173.89	90.65
aug-cc-pVDZ	MP2	1.0925	1.3314	1.3028	1.3164	1.1810	119.55	175.94	147.64	171.41	90.77
cc-pVTZ	MP2(fu)	1.0763	1.3096	1.2711	1.2807	1.1692	119.50	178.33	166.06	176.29	90.45
6-31G(d)	QCISD	1.0871	1.3170	1.2899	1.2981	1.1795	118.09	177.42	154.78	172.12	90.53
Prediction		1.08(1)	1.31(2)	1.27(2)	1.28(2)	1.17(1)	119.5(5)	179(1)	172(8)	178(2)	90.2(2)

[a]Bond lengths r in Å, bond angles θ in degrees. α, β, etc., denote carbon atoms counting from the oxygen end of the molecule.
[b](fu) means all electrons correlated; otherwise, the core electrons are frozen in the correlation treatments.
[c]τ_{HCCC} denotes the dihedral angle. The CH_2 group is bent in a *trans* fashion away from C_β.

TABLE IV. Minimum-energy (kinked, C_s symmetry) structures for H_2C_5O.[a,b]

Basis set	Method	r_{CH}^{trans}	r_{CH}^{cis}	$r_{\delta\varepsilon}$	$r_{\gamma\delta}$	$r_{\beta\gamma}$	$r_{\alpha\beta}$	r_{CO}	θ_{HCH}	θ_{HCC}^{trans}	θ_{HCC}^{cis}	θ_δ	θ_γ	θ_β	θ_α
6-31G(d)	HF	1.0769	1.0767	1.3039	1.2640	1.2784	1.2737	1.1498	117.00	121.38	121.61	179.52	178.96	165.84	176.09
6-31G(d)	MP2	1.0894	1.0899	1.3282	1.2774	1.3036	1.3042	1.1858	116.30	121.83	121.87	175.81	174.68	147.16	170.50
cc-pVDZ	MP2	1.0981	1.0988	1.3387	1.2888	1.3149	1.3184	1.1800	117.21	121.38	121.41	175.67	174.46	145.00	170.45
6-311G(d,p)	MP2	1.0891	1.0897	1.3291	1.2769	1.2999	1.3000	1.1736	117.10	121.39	121.51	174.45	174.28	150.35	172.13
cc-pVTZ	MP2(fu)	1.0807	1.0811	1.3189	1.2678	1.2803	1.2763	1.1728	117.20	121.44	121.36	176.96	177.83	171.65	177.53
6-31G(d)	QCISD	1.0901	1.0903	1.3252	1.2800	1.3003	1.3002	1.1810	116.69	121.64	121.67	177.61	176.28	152.00	170.69
Prediction		1.08(1)	1.08(1)	1.32(1)	1.27(2)	1.28(2)	1.28(2)	1.17(1)	117.5(5)	121.4(5)	121.4(5)	177(3)	178(2)	172(8)	177(3)

[a]Bond lengths r in Å, bond angles θ in degrees. α,β, etc., denote carbon atoms counting from the oxygen end of the molecule.
[b](fu) means all electrons correlated; otherwise, the core electrons are frozen in the correlation treatments.

MP2(fu)/PZ($3d2f,2p1d$) barriers minus the MP2/cc-pVTZ barriers] were -73 for H_2C_3O, -19 for H_2C_4O, and -10 for H_2C_5O.

Our best estimates for V_{eq} are 390–400 for H_2C_3O and $0-10$ cm^{-1} for H_2C_4O and H_2C_5O. The true values likely lie within 80 cm^{-1} of these. Naturally, for H_2C_4O and H_2C_5O the existence of the equilibrium potential barrier can be neither confirmed nor denied. Comparison to experimental values will be deferred to the discussion of zero-point vibrational effects in Sec. VI.

IV. EQUILIBRIUM GEOMETRIES

Several of the optimized kinked (C_s) structures of propadienone, butatrienone, and pentatetrenone, as well as our best-guess predictions, are found in Tables II, III, and IV, respectively. Our predictions incorporate the dependence of the coordinates upon the principal angles θ_β, which are determined to be 142 ± 3(H_2C_3O), 172 ± 8(H_2C_4O), and $172\pm8°$(H_2C_5O) from Fig. 2 and the barrier predictions of the previous section. While absolute predictions for individual bond lengths and angles are accurate to ~0.02 Å and 2°, respectively, *relative* bond lengths and angles are an order of magnitude more accurate, and we shall comment on these first.

A. CC bond lengths

Most noticeable is that the CC bond lengths vary upon their proximity to the methylene group and not the oxy group. The CC distance which involves the methylene carbon is generally 0.04 to 0.05 Å longer than the neighboring CC bond length, with ensuing damped oscillatory behavior. The various levels of theory are particularly consistent in this regard for the C_{2v} structures (not shown); for instance, all seven employed levels of theory used for C_{2v} pentatetrenone optimizations provided $r_{\alpha\beta}$ values smaller than $r_{\beta\gamma}$ ones by between 0.005 and 0.011 Å, despite the resonance figures which suggest a smaller bond order for $C_\alpha C_\beta$ than for $C_\beta C_\gamma$. With this consistency in mind, the various levels of theory could more properly be said to alter the carbon chain length rather than relative CC bond lengths, although the changes are more accentuated at the methylene end of the chain. The effect of cumulenone extension upon the $C{=}CH_2$ distance is oscillatory with a 0.01 Å range, it being the longest in H_2C_5O and the shortest in H_2C_4O. However, upon bending propadienone to its equilibrium position, the $C{=}CH_2$ distance increases 0.01 Å or more.

B. CO and CH bond lengths

The trend of r_{CO} with chain length is oscillatory on the scale of 0.002 Å, with the shortest r_{CO} value for H_2C_4O. The r_{CH} values also oscillate with increasing chain length, on the order of 0.01 Å at C_{2v}, but the large propadienone kink boosts its CH bond lengths another 0.01 Å or more.

C. Methylene HCH angle

Ketene (H_2CCO) is known to be unusual in that its methylene valence bond angle θ_{HCH} is greater than 120°, by almost 2°.[78] Formaldehyde (among many other molecules with $=CH_2$ moieties) does not have such an extended angle. From our results, no other cumulenone should have a methylene angle greater than 120° either. The series is clearly oscillatory from formaldehyde through to pentatetrenone, with predicted methylene angles of 116.5, 119.5, and 117.5° (to the best half-degree) for H_2C_3O through H_2C_5O.

D. Chain kink angles

For all three cumulenones, the kinks at locations other than C_β are proportionally smaller than the kink at C_β. For propadienone, the CCO angles (θ_α) at correlated levels of theory are between 164 and 170°, while the corresponding principal angles (θ_β) fall between 135 and 144°. We have found (for the first time, we believe) two HF kinked structures for propadienone, but they still misleadingly suggest an equilibrium structure close to C_{2v}. For H_2C_4O and H_2C_5O, the frozen-core MP2 results in this section give θ_α angles of 171–174 and 170–173°, respectively, with corresponding θ_β

TABLE V. Rotational constant predictions (GHz) and dipole moments μ (Debye).

	H_2C_3O		H_2C_4O		H_2C_5O
	Theory[a]	Expt[b]	Theory[a]	Expt[c]	Theory[a]
A	140(20)	153.6	270(30)	220[d]	250(60)
B	4.3(2)	4.387	2.16(5)	2.161	1.26(3)
C	4.2(2)	4.258	2.14(5)	2.147	1.25(3)
μ	2.9	2.30	2.6	1.97	4.1

[a]Theoretical predictions based on Tables II–IV for rotational constants; HF/cc-pVTZ values for dipole moments.
[b]Reference 35 for rotational constants; Ref. 32 for dipole moment.
[c]Reference 10 for rotational constants; Ref. 79 for dipole moment.
[d]Assumed value.

TABLE VI. Internal coordinate sets for vibrational analyses of cumulenones.[a]

$H_2C_\gamma C_\beta C_\alpha O$	$H_2C_\delta C_\gamma C_\beta C_\alpha O$	$H_2C_\varepsilon C_\delta C_\gamma C_\beta C_\alpha O$
Chain stretching modes		
$S_1=r_{CO}$	$S_1=r_{CO}$	$S_1=r_{CO}$
$S_2=r_{\alpha\beta}$	$S_2=r_{\alpha\beta}$	$S_2=r_{\alpha\beta}$
$S_3=r_{\beta\gamma}$	$S_3=r_{\beta\gamma}$	$S_3=r_{\beta\gamma}$
	$S_4=r_{\gamma\delta}$	$S_4=r_{\gamma\delta}$
		$S_5=r_{\delta\epsilon}$
Hydrogen motions		
$S_4=2^{-1/2}[r_{CH_a}+r_{CH_b}]$	$S_5=2^{-1/2}[r_{CH_a}+r_{CH_b}]$	$S_6=2^{-1/2}[r_{CH_a}+r_{CH_b}]$
$S_5=2^{-1/2}[r_{CH_a}-r_{CH_b}]$	$S_6=2^{-1/2}[r_{CH_a}-r_{CH_b}]$	$S_7=2^{-1/2}[r_{CH_a}-r_{CH_b}]$
$S_6=2^{-1/2}[\beta_{CCH_a}+\beta_{CCH_b}]$	$S_7=2^{-1/2}[\beta_{CCH_a}+\beta_{CCH_b}]$	$S_8=2^{-1/2}[\beta_{CCH_a}+\beta_{CCH_b}]$
$S_7=2^{-1/2}[\beta_{CCH_a}-\beta_{CCH_b}]$	$S_8=2^{-1/2}[\beta_{CCH_a}-\beta_{CCH_b}]$	$S_9=2^{-1/2}[\beta_{CCH_a}-\beta_{CCH_b}]$
$S_8=\gamma(_{CCH_2})$	$S_9=\gamma(_{CCH_2})$	$S_{10}=\gamma(_{CCH_2})$
Chain bending modes		
$S_9=2^{-1/2}[\theta_x^{a\gamma\beta\alpha}-\theta_x^{b\gamma\beta\alpha}]$	$S_{10}=2^{-1/2}[\theta_x^{a\delta\gamma\beta}-\theta_x^{b\delta\gamma\beta}]$	$S_{11}=2^{-1/2}[\theta_x^{a\epsilon\delta\gamma}-\theta_x^{b\epsilon\delta\gamma}]$
$S_{10}=2^{-1/2}[\theta_x^{a\gamma\alpha O}-\theta_x^{b\gamma\alpha O}]$	$S_{11}=2^{-1/2}[\theta_x^{a\delta\beta\alpha}-\theta_x^{b\delta\beta\alpha}]$	$S_{12}=2^{-1/2}[\theta_x^{a\epsilon\gamma\beta}-\theta_x^{b\epsilon\gamma\beta}]$
$S_{11}=2^{-1/2}[\theta_y^{a\gamma\beta\alpha}-\theta_y^{b\gamma\beta\alpha}]$	$S_{12}=2^{-1/2}[\theta_x^{a\delta\alpha O}-\theta_x^{b\delta\alpha O}]$	$S_{13}=2^{-1/2}[\theta_x^{a\epsilon\beta\alpha}-\theta_x^{b\epsilon\beta\alpha}]$
$S_{12}=2^{-1/2}[\theta_y^{a\gamma\alpha O}-\theta_y^{b\gamma\alpha O}]$	$S_{13}=2^{-1/2}[\theta_y^{a\delta\gamma\beta}-\theta_y^{b\delta\gamma\beta}]$	$S_{14}=2^{-1/2}[\theta_x^{a\epsilon\alpha O}-\theta_x^{b\epsilon\alpha O}]$
$S_{14}=2^{-1/2}[\theta_y^{a\delta\beta\alpha}-\theta_y^{b\delta\beta\alpha}]$	$S_{15}=2^{-1/2}[\theta_y^{a\epsilon\delta\gamma}-\theta_y^{b\epsilon\delta\gamma}]$	
	$S_{15}=2^{-1/2}[\theta_y^{a\delta\alpha O}-\theta_y^{b\delta\alpha O}]$	$S_{16}=2^{-1/2}[\theta_y^{a\epsilon\gamma\beta}-\theta_y^{b\epsilon\gamma\beta}]$
		$S_{17}=2^{-1/2}[\theta_y^{a\epsilon\beta\alpha}-\theta_y^{b\epsilon\beta\alpha}]$
		$S_{18}=2^{-1/2}[\theta_y^{a\epsilon\alpha O}-\theta_y^{b\epsilon\alpha O}]$

[a]Definitions are the same as in Ref. 78: r_{AB} in the $A-B$ interatomic distance; β_{ABC} is the angle between bond directions $B-A$ and $B-C$; the β_{CCH_a} and $\gamma(_{CCH_2})$ designations assume the two carbon atoms nearest the hydrogens; $\gamma(_{CCH_2})$ is the angle between the C–C bond vector and the methylene plane; and θ_x^{ijkl} and θ_y^{ijkl} are the in-plane and out-of-plane dimensionless linear bending coordinates, which measure the components of the unit vector of the $k-l$ bond perpendicular to the $j-k$ axis. Note that j and k are not necessarily neighboring atoms. Atom i defines the ijk plane and the direction of positive displacement.

angles of 147–156 and 145–151°. Optimum CCC angles (other than the principal angle) are always less kinked than the CCO segment.

The only related experiment-based structures are the ones for propadienone from R. D. Brown and co-workers.[11,35] Their semirigid bender (SRB) analysis[11] used spectral fitting to generate only potential function parameters; geometrical parameters were manually adjusted, guided by observed rotational constants, some *ab initio* information, and intuition. Hence the two SRB-derived structures we quote do not directly arise from the rotational spectral lines, and will not be as accurate as the SRB structures of smaller molecules. The substitution (r_s) structure[35] arises from the rotational constants of isotopically substituted versions of the molecule, and may be more accurate in this case.

Our predictions for the rotational constants, based on the best-guess geometrical predictions, appear in Table V. The B and C constants are mostly dependent on chain length, while the large A constant is mostly dependent, and very sensitive to, the extent of kink in the carbon chain. Values of 285–295 GHz for A would be indicative of linear structures for H_2C_4O and H_2C_5O. Experimentally, rotational constants were determined from microwave spectra by R. D. Brown and co-workers, who generated short-lived gas-phase propadienone[35] and butatrienone[10] by flash vacuum pyrolysis of anhydride precursors. The agreement is very good, acknowledging that the theoretical ones relate to equilibrium (r_e) geometries while the experimental ones relate to ground-state-averaged (r_0) geometries. Dipole moments were only calculated here with HF theory, and appear to be larger than experiment[32,79] by 0.6 Debye; we therefore naïvely predict the unknown dipole moment for gas-phase pentatetrenone to be 3.5 Debye.

V. VIBRATIONAL ANALYSIS

In this work, MP2/6-31G(d) harmonic force fields were computed analytically for H_2C_3O, H_2C_4O, and H_2C_5O, at their C_s minima and their C_{2v} stationary points. The MP2/6-31G(d) harmonic frequencies for C_s H_2C_3O have already been published.[80] A variety of different sets of internal coordinates were tested for the total energy distribution (TED) analysis of the normal modes, primarily because several of the normal modes are delocalized throughout the molecule, and in such cases one has the option of either simple internal coordinates and a multicomponent TED, or combined internal coordinates and a simple TED. Our chosen set, displayed in Table VI, employs simple (localized) internal coordinates which can be applied to both C_s and C_{2v} symmetries.

The complete vibrational analyses and the MP2/6-31G(d) harmonic vibrational frequencies for the three cumulenones are displayed in Tables VII–IX. The numbering of the modes is according to C_s symmetry for H_2C_3O, but C_{2v} for H_2C_4O and H_2C_5O.

For propadienone (Table VII), the optimized C_{2v} structure is a transition state for in-plane bending, and produces an imaginary frequency for the floppy vibration ν_9. The C_s minimum produces all positive frequencies, and according to the TED the floppy mode at the C_s minimum is essentially

TABLE VII. Harmonic fundamental vibrational frequency analysis for H_2C_3O.[a]

Mode	Description	ω_i	ν_i(expt)[b]	IR intensity	TED[c]
C_{2v}					
$\nu_9(b_2)$	bend, in-plane	166*i*		(17.9)	$S_9(98.7)$
$\nu_{12}(b_1)$	bend, out-of-plane	224		0.1	$S_{12}(51.1)+S_{11}(49.4)$
$\nu_8(b_2)$	bend, in-plane	439	479	12.5	$S_{10}(96.2)$
$\nu_{11}(b_1)$	bend, out-of-plane	632	674	18.5	$S_{11}(51.8)-S_{12}(48.6)$
$\nu_7(a_1)$	chain osc.	925	910	2.8	$S_2(44.8)+S_3(34.3)+S_1(19.2)$
$\nu_{10}(b_1)$	CH_2 wag	1021	988	25.5	$S_8(100.9)$
$\nu_6(b_2)$	CH_2 rock	1094	1047	1.2	$S_7(100.5)$
$\nu_5(a_1)$	CH_2 scissor	1527	1457	5.4	$S_6(94.4)-S_1(4.1)$
$\nu_4(a_1)$	chain osc.	1789	1685	10.7	$S_3(52.5)-S_1(39.8)-S_6(4.3)$
$\nu_3(a_1)$	chain osc.	2340	2124	651.3	$S_2(50.5)-S_1(36.9)-S_3(12.7)$
$\nu_2(a_1)$	CH sym. stretch	3149	2968,2978	25.8	$S_4(99.7)$
$\nu_1(b_2)$	CH antisym. stretch	3225	3026,3037	12.0	$S_5(100.0)$
C_s					
$\nu_9(a')$	bend, in-plane	205		17.6	$S_9(72.7)+S_{10}(28.8)$
$\nu_{12}(a'')$	bend, out-of-plane	279		4.6	$S_{12}(74.1)+S_{11}(26.2)$
$\nu_8(a')$	bend, in-plane	515	479	10.7	$S_{10}(71.4)-S_9(31.6)$
$\nu_{11}(a'')$	bend, out-of-plane	710	674	8.1	$S_{11}(75.0)-S_{12}(25.6)$
$\nu_7(a')$	chain osc.	961	910	1.6	$S_2(56.0)+S_3(25.4)+S_1(16.4)-S_7(5.0)$
$\nu_{10}(a'')$	CH_2 wag	1022	988	27.4	$S_8(100.9)$
$\nu_6(a')$	CH_2 rock	1109	1047	22.3	$S_7(94.3)$
$\nu_5(a')$	CH_2 scissor	1530	1457	1.4	$S_6(88.8)$
$\nu_4(a')$	chain osc.	1735	1685	6.6	$S_3(63.4)-S_1(19.4)-S_6(10.1)-S_2(6.9)$
$\nu_3(a')$	chain osci.	2207	2124	617.3	$S_1(59.3)-S_2(35.1)+S_3(5.4)$
$\nu_2(a')$	CH sym. stretch	3163	2968,2978	22.8	$S_4(95.7)$
$\nu_1(a')$	CH antisym. stretch	3251	3026,3037	10.3	$S_5(96.1)$

[a]Frequencies in cm^{-1}, IR intensities in km mol^{-1}.

[b]Nitrogen-matrix results of Ref. 40, but assignments are ours. Four of their tabulated peaks must not be fundamentals of propadienone. The CH stretching doublets are perhaps due to aggregation formed during deposition of the matrix; see their discussion of the splitting of the peak at 2125 cm^{-1}.

[c]Total energy distributions. In the $S_n(k_n)$ notation, the n refers to the internal coordinate (see Table VI) and k_n is its contribution (values have been multiplied by 100) to the normal mode.

bending at the beta carbon (bending of the $C_\alpha C_\beta$ vector from the $C_\beta C_\gamma$ axis). The most infrared-intense fundamental is the maximally antisymmetric chain oscillation ν_3. Comparisons between the C_{2v} and C_s results are akin to observing effects of traversing the double-well potential of the floppy mode from its maximum to one of the minima. The two heavy-atom out-of-plane bending modes have coupled the bending at two apex carbon atoms, with this coupling nearly equal at C_{2v} but reduced once the in-plane θ_β angle has been bent to 138°. All but two of the non-ν_9 frequencies rise upon bending toward the minimum, these two being the high-frequency chain oscillations which at C_{2v} receive the greatest contribution from the $r_{\alpha\beta}$ and $r_{\beta\gamma}$ bond stretches. Since these two bond lengths are the only ones which lengthen as the molecule is bent at the beta carbon, it is quite understandable that only two stretching frequencies will drop. Note from the TEDs that the three chain stretching modes largely hold their character whether θ_β is 180 or 138°, although a somewhat localized CO stretch is apparent for the C_s structure.

Two matrix-isolated infrared absorption spectra of propadienone were obtained and reported by Chapman, Miller, and Pitzenberger in 1987.[40] The differences between the argon-matrix and nitrogen-matrix frequencies are less than 15 cm^{-1}. They refrained from making assignments, and in fact four of their listed peaks are not due to fundamentals of propadienone, based on our results. Our assignments are quite straightforward, using the application of the usual scale factor of 0.94 to convert MP2/6-31G(d) harmonic frequencies to approximate fundamentals.

For butatrienone (Table VIII), the optimized C_{2v} structure is a transition state, but for out-of-plane bending; note the b_1 symmetry of the floppy vibration ν_{10}. This mode shows an imaginary harmonic frequency at C_{2v} and a small harmonic at the C_s minimum; the TED demonstrates that (as in propadienone) the floppy mode is substantially bending at C_β but (unlike propadienone) in a perpendicular direction from the methylene plane. The most infrared-intense fundamental is again the maximally antisymmetric chain oscillation ν_2. Most chain-bending modes involve concerted motions at more than one apex, even at the C_s minimum ($\theta_\beta = 150°$). All but four of the non-ν_{10} frequencies rise upon bending toward the minimum; two of the four which drop are, as in H_2C_3O, the high-frequency chain oscillations which at C_{2v} receive the greatest contribution from the $r_{\alpha\beta}$ and $r_{\beta\gamma}$ bond stretches. The other two have dominant energetic contributions from the CH_2 scissoring motion; for propadienone the scissor harmonic frequency rises upon bending, but only 3 cm^{-1} for a displacement of 42 deg. The CH_2 scissor vibration in H_2C_4O is mixed with a chain oscillation which is very much localized to the methylene end of the molecule. Despite this, the chain stretching modes largely hold their character upon bending, and no localized CO stretch is apparent for the C_s structure.

Argon-matrix infrared absorption spectra of butatrienone

TABLE VIII. Harmonic fundamental vibrational frequency analysis for H_2C_4O.[a]

Mode	Description	ω_i	ν_i(expt)[b]	IR intensity	TED[c]
C_{2v}					
$\nu_{10}(b_1)$	bend, out-of-plane	137*i*		(8.3)	$S_{14}(91.4)+S_{15}(8.4)$
$\nu_{15}(b_2)$	bend, in-plane	147		0.0012	$S_{11}(53.6)+S_{12}(42.8)$
$\nu_9(b_1)$	bend, out-of-plane	348		15.3	$S_{13}(62.2)+S_{15}(44.3)-S_{14}(-4.4)$
$\nu_{14}(b_2)$	bend, in-plane	407		0.3	$S_{10}(80.7)+S_8(12.7)-S_{12}(7.7)$
$\nu_8(b_1)$	bend, out-of-plane	495		5.3	$S_{15}(47.3)-S_{13}(40.8)-S_{14}(12.8)$
$\nu_{13}(b_2)$	bend, in-plane	614		21.2	$S_{12}(49.6)-S_{11}(47.3)$
$\nu_7(b_1)$	CH_2 wag	706	728	90.9	$S_9(102.1)$
$\nu_6(a_1)$	chain osc.	760		0.5	$S_2(34.0)+S_3(33.5)+S_4(19.5)+S_1(11.7)$
$\nu_{12}(b_2)$	CH_2 rock	998		4.2	$S_8(86.4)-S_{10}(13.7)$
$\nu_5(a_1)$	CH_2 scissor	1392		4.6	$S_7(67.2)+S_4(13.3)-S_1(9.7)-S_2(9.4)$
$\nu_4(a_1)$	chain osc.	1530	1456,1495	58.0	$S_4(35.8)-S_7(31.8)-S_1(17.0)-S_2(10.4)$
$\nu_3(a_1)$	chain osc.	2069	1996	5.8	$S_3(38.9)-S_1(31.5)-S_4(28.3)$
$\nu_2(a_1)$	chain osc.	2379	2242	1712.4	$S_2(44.9)-S_1(30.1)-S_3(22.5)$
$\nu_1(a_1)$	CH sym. stretch	3215	3035	23.0	$S_5(99.5)$
$\nu_{11}(b_2)$	CH antisym. stretch	3306	3105	1.5	$S_6(100.2)$
C_s					
$\nu_{10}(a')$	bend, out-of-plane[d]	91		3.6	$S_{14}(74.3)+S_{15}(27.0)$
$\nu_{15(a'')}$	bend, in-plane	193		1.9	$S_{12}(52.3)+S_{11}(44.6)$
$\nu_{14}(a'')$	bend, in-plane	403		0.2	$S_{10}(81.5)+S_8(12.4)-S_{12}(7.8)$
$\nu_9(a')$	bend, out-of-plane	466		15.8	$S_{13}(61.1)+S_{15}(26.9)-S_{14}(15.1)$
$\nu_8(a')$	bend, out-of-plane	502		10.4	$S_{15}(46.2)-S_{13}(40.8)-S_{14}(13.4)$
$\nu_{13}(a'')$	bend, in-plane	629		19.7	$S_{11}(57.1)-S_{12}(40.1)$
$\nu_7(a')$	CH_2 wag	729	728	93.6	$S_9(101.5)$
$\nu_6(a')$	chain osc.	805		2.6	$S_2(38.6)+S_3(34.4)+S_4(18.5)+S_1(10.3)$
$\nu_{12}(a'')$	CH_2 rock	1000		3.8	$S_8(86.7)-S_{10}(13.6)$
$\nu_5(a')$	CH_2 scissor	1385		3.0	$S_7(58.2)+S_4(16.6)-S_2(13.1)-S_1(11.1)$
$\nu_4(a')$	chain osc.	1517	1456,1495	29.9	$S_7(40.6)-S_4(29.3)+S_1(13.0)+S_2(10.3)$
$\nu_3(a')$	chain osc.	2064	1996	37.2	$S_3(40.8)-S_4(31.7)-S_1(26.7)$
$\nu_2(a')$	chain osc.	2312	2242	1506.0	$S_2(40.4)-S_1(38.1)-S_3(18.6)$
$\nu_1(a')$	CH sym. stretch	3216	3035	21.2	$S_5(99.5)$
$\nu_{11}(a'')$	CH antisym. stretch	3306	3105	1.5	$S_6(100.2)$

[a]See Table VII.
[b]Argon-matrix results of Ref. 41. A Fermi resonance doublet occurs (1456 and 1495 cm^{-1}) due to resonance between the ν_4 fundamental and an overtone or combination band.
[c]See Table VII.
[d]The ''plane'' for H_2C_4O is that of the methylene group, not the C_s symmetry plane.

were taken by R. F. C. Brown and co-workers and reported in 1990.[41] We take their assignments in listing their fundamentals in Table VIII. We agree with their discussion concerning the pair at 1456 and 1495 cm^{-1}, being a Fermi resonance with a nonfundamental level, possibly 2 ν_6 or $\nu_{12}\nu_{13}$. The assignment of the methylene wag to the 728 cm^{-1} band is based on intensity, and despite the apparent low value of the MP2/6-31G(d) harmonic (729 for C_s and 706 cm^{-1} for C_{2v} *before* scaling), this mode is expected to receive a positive contribution from Coriolis effects, which for ketene outweighed the negative anharmonic contribution due to higher order derivatives of the potential energy surface.[78]

For H_2C_5O, (Table IX), the floppy vibration ν_{18} is an in-plane bend which presents an imaginary harmonic frequency at C_{2v} and a small harmonic at the C_s minimum; the TED demonstrates again (as in H_2C_3O and H_2C_4O) that the floppy mode is substantially bending at C_β. Again the most infrared-intense fundamental is the maximally antisymmetric chain oscillation mode ν_2. The other in-plane chain-bending modes can be assigned to bending at one apex. The out-of-plane chain-bending modes are somewhat localized into two *trans* modes and two *cis* modes, the *trans* ones being of higher frequency. All but seven of the non-ν_{18} frequencies rise upon bending from the C_{2v} transition state to the minimum; two are virtually unchanged and five drop. It is much more difficult to argue that two frequencies drop due to the elongation of the $r_{\alpha\beta}$ and $r_{\beta\gamma}$ optimized lengths. Three of the five chain oscillation frequencies drop, and only one (the chain breathing mode) rises upon bending to the minimum ($\theta_\beta = 147°$). The other two modes which drop are the methylene wag and scissor, by 8 and 12 cm^{-1}, respectively. The chain stretching modes hold their character upon bending, and no localized CO stretch is apparent.

Efforts to synthesize pentatetrenone and obtain argon-matrix infrared absorption spectra were made by R. F. C. Brown and co-workers and reported in 1988.[42] They found three peaks which they tentatively assigned to pentatetrenone, the most intense one being the best evidence for the success of their syntheses. Their argon-matrix peaks for the most populous isotopomer are in reasonable accord with the approximate 0.94 scaling of our gas-phase computed values. To examine their ^{13}C-substitution frequency shifts, we performed an additional normal mode analysis on the MP2/6-31G(d) harmonic force field of C_s and C_{2v} pentatetrenone, with ^{13}C substituted at the carbonyl (C_α) position. Our unscaled ^{13}C shifts (in $cm^{-}1$) for $\{\nu_2, \nu_3, \nu_4\}$ are

TABLE IX. Harmonic fundamental vibration frequency analysis for H_2C_5O.[a]

Mode	Description	ω_i	ν_i(expt)[b]	IR intensity	TED[c]
C_{2v}					
$\nu_{18}(b_2)$	bend, in-plane	169_i		(13.0)	$S_{13}(88.6)+S_{11}(10.3)$
$\nu_{12}(b_2)$	bend, out-of-plane	105		0.2	$S_{17}(51.4)+S_{18}(36.0)+S_{16}(9.2)$
$\nu_{17}(b_2)$	bend, in-plane	159		3.2	$S_{11}(81.9)+S_{12}(13.6)$
$\nu_{16}(b_2)$	bend, in-plane	233		8.0	$S_{12}(72.3)+S_{14}(31.4)-S_{13}(-8.8)-S_{11}(4.8)$
$\nu_{11}(b_1)$	bend, out-of-plane	275		1.7	$S_{16}(48.5)+S_{15}(36.5)-S_{18}(12.7)$
$\nu_{15}(b_2)$	bend, in-plane	471		7.3	$S_{14}(64.5)-S_{13}(17.5)-S_{12}(15.9)$
$\nu_{10}(b_1)$	bend, out-of-plane	482		5.1	$S_{15}(58.9)-S_{16}(42.1)$
$\nu_9(b_1)$	bend, out-of-plane	591		14.6	$S_{18}(51.3)-S_{17}(46.6)$
$\nu_7(a_1)$	chain osc.	643		0.6	$S_3(32.3)+S_2(24.1)+S_4(23.2)+S_5(12.2)$
$\nu_8(b_1)$	CH_2 wag	953		37.8	$S_{10}(100.9)$
$\nu_{14}(b_2)$	CH_2 rock	1063		0.1	$S_9(98.7)$
$\nu_6(a_1)$	chain osc.	1240		12.4	$S_5(35.4)-S_2(23.4)-S_1(17.4)+S_4(15.6)$
$\nu_5(a_1)$	CH_2 scissor	1517		0.9	$S_8(91.4)$
$\nu_4(a_1)$	chain osc.	1793	1726	53.3	$S_5(34.3)-S_3(29.9)+S_1(27.1)-S_4(4.7)$
$\nu_3(a_1)$	chain osc.	2174	2068	27.3	$S_4(49.7)-S_5(16.5)+S_1(15.5)-S_3(15.1)$
$\nu_2(a_1)$	chain osc.	2354	2207	1961.4	$S_2(45.3)-S_1(29.9)-S_3(20.6)$
$\nu_1(a_1)$	CH sym. stretch	3163		10.9	$S_6(99.7)$
$\nu_{13}(b_2)$	CH antisym. stretch	3244		4.6	$S_7(100.1)$
C_s					
$\nu_{18}(a')$	bend, in-plane	83		3.4	$S_{13}(65.5)+S_{14}(29.6)$
$\nu_{12}(a'')$	bend, out-of-plane	170		2.0	$S_{18}(40.3)+S_{17}(36.1)+S_{16}(17.9)+S_{15}(5.8)$
$\nu_{17}(a')$	bend, in-plane	189		2.3	$S_{11}(75.8)+S_{12}(17.8)$
$\nu_{11}(a'')$	bend, out-of-plane	266		2.4	$S_{16}(44.1)+S_{15}(31.3)-S_{18}(21.9)$
$\nu_{16}(a')$	bend, in-plane	393		14.4	$S_{12}(74.8)-S_{11}(19.5)-S_{13}(5.9)$
$\nu_{15}(a')$	bend, in-plane	485		9.0	$S_{14}(66.5)-S_{13}(27.7)-S_{12}(4.6)$
$\nu_{10}(a'')$	bend, out-of-plane	566		1.9	$S_{15}(63.2)-S_{16}(33.2)+S_{18}(4.7)$
$\nu_9(a'')$	bend, out-of-plane	612		18.1	$S_{17}(61.5)-S_{18}(33.1)-S_{16}(4.5)$
$\nu_7(a')$	chain osc.	699		3.9	$S_3(33.6)+S_2(28.3)+S_4(22.7)+S_5(12.7)$
$\nu_8(a'')$	CH_2 wag	945		38.4	$S_{10}(100.9)$
$\nu_{14}(a')$	CH_2 rock	1062		0.3	$S_9(98.5)$
$\nu_6(a')$	chain osc.	1228		3.5	$S_5(32.8)-S_2(29.2)-S_1(16.5)+S_4(15.1)$
$\nu_5(a')$	CH_2 scissor	1512		1.2	$S_8(91.4)$
$\nu_4(a')$	chain osc.	1768	1726	17.8	$S_5(35.7)-S_3(34.9)+S_1(20.4)$
$\nu_3(a')$	chain osc.	2174	2068	22.7	$S_4(48.9)+S_1(17.5)-S_5(16.8)-S_3(12.9)$
$\nu_2(a')$	chain osc.	2280	2207	1742.5	$S_2(37.5)-S_1(36.5)-S_3(18.1)+S_4(7.0)$
$\nu_1(a')$	CH sym. stretch	3166		9.4	$S_6(99.6)$
$\nu_{13}(a')$	CH antisym. stretch	3248		3.9	$S_7(100.0)$

[a]See Table VII.
[b]Argon-matrix results of Ref. 42.
[c]See Table VII.

$\{-38,-15,-7\}$ for C_{2v} and $\{-36,-20,-5\}$ for C_s, in excellent agreement with the observed results of $\{-39,-12,-6\}$. This work provides substantial support for the identification of pentatetrenone in their pyrolysis products.

VI. ZERO-POINT VIBRATIONAL EFFECTS

The floppiest bending mode operates on a potential determined not only by electronic and nuclear repulsion energies, but by zero-point vibrational energies (ZPVE) of the other vibrational modes as well. Their inclusion gives rise to an effective potential function for the principal bending mode (Fig. 6), with its own minimum θ_{eff} and barrier height V_{eff} which are normally predicted very well by θ_{eq} and V_{eq}. However, the V_{eq} for H_2C_4O and H_2C_5O appear so small that θ_{eq} and θ_{eff} could differ on the order of a few degrees, and since the semirigid bender results correspond better to θ_{eff} than to θ_{eq} a brief discussion is offered here.

The usual way of approximating V_{eff} from *ab initio* data (V^*_{eff}) is simply to add the difference in ZPVE (not including the ZPVE contribution of the bending mode in question) to the equilibrium barrier V_{eq}. The better way (V^{**}_{eff}) is identical, except that the electronic and ZPVE energies for the C_s form are computed at the minimum (θ_{eff}) on the ZPVE-corrected potential surface. The *ab initio* approximation to the angle θ_{eff} is denoted θ^*_{eff} and is computed by minimizing not only $E_{\text{elec}}+V_{nn}$ along the bending mode of interest, but $E_{\text{elec}}+V_{nn}+\text{ZPVE}$, where the ZPVE contribution of the floppy bend is omitted. The usual quantity $E_{\text{elec}}+V_{nn}$, the sum of electronic and internuclear repulsion energies, is the one minimized along the other internal coordinates. The ''better way'' is rarely attempted, however, and for good reason; we tested this method for each cumulenone at the MP2/6-31G(d) level of theory, and found the magnitude of improvement to be less than the accuracy of typical ZPVE corrections.

Employing the usual method, then, the ZPVE corrections for $V_{\text{eq}}\rightarrow V^*_{\text{eff}}$ (using the MP2/6-31G(d) harmonic frequencies of Sec. V) are -55, -76, and $-142\ \text{cm}^{-1}$ for

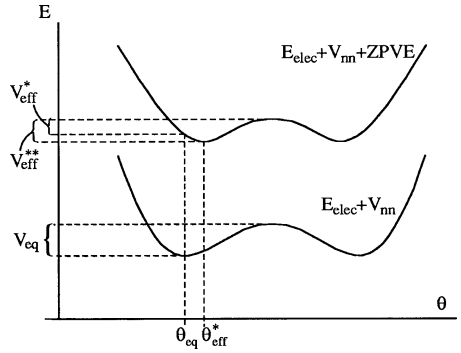

FIG. 6. Diagram demonstrating features on the one-dimensional potential surface for a double-well floppy mode. $E_{\mathrm{elec}}+V_{nn}$: the equilibrium (vibrationless) potential for nuclear motion. $E_{\mathrm{elec}}+V_{nn}+\mathrm{ZPVE}$: an effective potential arising from the approximation of adiabatic separation of this mode from the higher frequency modes, which contribute their zero-point vibrational energies (ZPVE) to this potential.

H_2C_3O, H_2C_4O, and H_2C_5O, respectively. These are quite approximate [the MP2(fu)/cc-pVTZ result for H_2C_3O is $-96\ \mathrm{cm}^{-1}$, and anharmonicity is neglected], but certainly provide stronger evidence that (i) H_2C_4O and H_2C_5O have *effective* C_{2v} minima, and (ii) H_2C_3O has an effective barrier to chain linearity of roughly $325\pm80\ \mathrm{cm}^{-1}$. This is in agreement with the semirigid bender V_{eff} values of R. D. Brown and co-workers[10,11] ($359\ \mathrm{cm}^{-1}$ for H_2C_3O and zero for H_2C_4O).

VII. CONCLUSIONS

Propadienone (H_2C_3O), butatrienone (H_2C_4O), and pentatetrenone (H_2C_5O) each have a floppiest carbon–chain bending mode which involves all-*trans* (zigzag) kinking, but most significantly a kink at the beta carbon. Their equilibrium barriers to linearity are estimated to be 400 ± 80, <80, and $<80\ \mathrm{cm}^{-1}$, respectively. Effective barriers (after zero-point effects are included) are $325\pm80\ \mathrm{cm}^{-1}$ for H_2C_3O and zero for H_2C_4O, bringing theory into agreement with the semirigid bender results of R. D. Brown and co-workers.[10,11] Equilibrium kinks for H_2C_4O and H_2C_5O can neither be confirmed nor denied. Our vibrational analysis strongly supports the detection by R. F. C. Brown and co-workers[42] of the highly reactive pentatetrenone molecule in the laboratory.

ACKNOWLEDGMENTS

Dr. A. P. Scott and Professor L. Radom are thanked for providing some of the geometry optimization data and for their hospitality and numerous fruitful discussions during the course of this work. Professor Radom and the Australian National University are also thanked for provision of a postdoctoral fellowship and computer resources.

[1] P. R. Bunker and B. M. Landsberg, J. Mol. Spectrosc. **67**, 374 (1977).
[2] P. R. Bunker, B. M. Landsberg, and B. P. Winnewisser, J. Mol. Spectrosc. **74**, 9 (1979).
[3] P. R. Bunker, J. Mol. Spectrosc. **80**, 422 (1980).
[4] M. Kreglewski, J. Mol. Struct. **60**, 105 (1980).
[5] Ch. V. S. Ramachandra Rao, J. Mol. Spectrosc. **89**, 197 (1981).
[6] P. Jensen and P. R. Bunker, J. Mol. Spectrosc. **94**, 114 (1982).
[7] P. Jensen, J. Mol. Spectrosc. **101**, 422 (1983).
[8] R. D. Brown, P. D. Godfrey, and B. Kleibömer, J. Mol. Spectrosc. **114**, 257 (1985).
[9] R. D. Brown, P. D. Godfrey, and B. Kleibömer, J. Mol. Spectrosc. **118**, 317 (1986).
[10] R. D. Brown, P. D. Godfrey, M. J. Ball, S. Godfrey, D. McNaughton, M. Rodler, B. Kleibömer, and R. Champion, J. Am. Chem. Soc. **108**, 6534 (1986).
[11] R. D. Brown, P. D. Godfrey, and R. Champion, J. Mol. Spectrosc. **123**, 93 (1987).
[12] M. Kreglewski, J. Mol. Spectrosc. **133**, 10 (1989).
[13] R. Champion, P. D. Godfrey, and F. L. Bettens, J. Mol. Spectrosc. **147**, 488 (1991).
[14] P. Jensen, P. R. Bunker, V. C. Eps, and A. Karpfen, J. Mol. Spectrosc. **151**, 384 (1992).
[15] R. Champion, P. D. Godfrey, and F. L. Bettens, J. Mol. Spectrosc. **155**, 18 (1992).
[16] P. Pracna, M. Winnewisser, and B. P. Winnewisser, J. Mol. Spectrosc. **162**, 127 (1993).
[17] S. C. Ross, M. Niedenhoff, and K. M. T. Yamada, J. Mol. Spectrosc. **164**, 432 (1994).
[18] D. McNaughton and S. C. Ross, J. Mol. Struct. **348**, 221 (1995).
[19] L. Farnell, R. Nobes, and L. Radom, J. Mol. Spectrosc. **93**, 271 (1982).
[20] J. H. Teles, G. Maier, B. A. Hess, Jr., L. J. Schaad, M. Winnewisser, and B. P. Winnewisser, Chem. Ber. **122**, 753 (1989).
[21] M. T. Nguyen, K. Pierloot, and L. G. Vanquickenborne, Chem. Phys. Lett. **181**, 83 (1991).
[22] A. P. Rendell, T. J. Lee, and R. Lindh, Chem. Phys. Lett. **194**, 84 (1992).
[23] N. C. Handy, C. W. Murray, and R. D. Amos, Philos. Mag. B **69**, 755 (1994).
[24] J. Koput, B. P. Winnewisser, and M. Winnewisser, Chem. Phys. Lett. **255**, 357 (1996).
[25] W. H. Weber, J. Mol. Spectrosc. **79**, 396 (1980).
[26] R. L. Lozes, J. R. Sabin, and J. Oddershede, J. Mol. Spectrosc. **86**, 357 (1981).
[27] L. J. Weimann and R. E. Christoffersen, J. Am. Chem. Soc. **95**, 2074 (1973).
[28] R. D. Amos, Chem. Phys. Lett. **108**, 347 (1984).
[29] P. Pyykko and N. Runeberg, J. Mol. Struct.: THEOCHEM **80**, 279 (1991).
[30] G. Trinquier and J.-P. Malrieu [J. Am. Chem. Soc. **109**, 5303 (1987)] presented an interesting argument for the bent nature of cumulenones based on the electronic singlet–triplet gaps of CO and H_2C_{n-1}.
[31] G. L. Blackman, R. D. Brown, R. F. C. Brown, F. W. Eastwood, and G. L. McMullen, J. Mol. Spectrosc. **68**, 488 (1977).
[32] R. D. Brown, P. D. Godfrey, R. Champion, and D. McNaughton, J. Am. Chem. Soc. **103**, 5711 (1981).
[33] R. D. Brown, P. D. Godfrey, R. Champion, and D. McNaughton, J. Am. Chem. Soc. **104**, 6167 (1982).
[34] R. D. Brown, J. Mol. Struct. **97**, 293 (1983).
[35] R. D. Brown, R. Champion, P. S. Elmes, and P. D. Godfrey, J. Am. Chem. Soc. **107**, 4109 (1985).
[36] L. Radom, Aust. J. Chem. **31**, 1 (1978).
[37] A. Komornicki, C. E. Dykstra, M. A. Vincent, and L. Radom, J. Am. Chem. Soc. **103**, 1652 (1981).
[38] L. Farnell and L. Radom, Chem. Phys. Lett. **91**, 373 (1982).
[39] L. Farnell and L. Radom, J. Am. Chem. Soc. **106**, 25 (1984).
[40] O. L. Chapman, M. D. Miller, and S. M. Pitzenberger, J. Am. Chem. Soc. **109**, 6867 (1987).
[41] R. F. C. Brown, K. J. Coulston, F. W. Eastwood, A. D. E. Pullin, and A. C. Staffa, Aust. J. Chem. **43**, 561 (1990).
[42] R. F. C. Brown, K. J. Coulston, F. W. Eastwood, M. J. Irvine, and A. D. E. Pullin, Aust. J. Chem. **41**, 225 (1988).
[43] W. J. Hehre, L. Radom, P. v. R. Schleyer, and J. A. Pople, *Ab Initio Molecular Orbital Theory* (Wiley, New York, 1986).
[44] (a) M. J. Frisch, G. W. Trucks, M. Head-Gordon, P. M. W. Gill, M. W. Wong, J. B. Foresman, B. G. Johnson, H. B. Schlegel, M. A. Robb, E. S. Replogle, R. Gomperts, J. L. Andres, K. Raghavachari, J. S. Binkley, C. Gonzalez, R. L. Martin, D. J. Fox, D. J. DeFrees, J. Baker, J. J. P. Stewart, and J. A. Pople, GAUSSIAN 92, Gaussian, Inc., Pittsburgh PA, 1992. (b) M. J. Frisch, G. W. Trucks, H. B. Schlegel, P. M. W. Gill, B. G. Johnson, M. A. Robb, J. R. Cheeseman, T. A. Keith, G. A. Petersson, J. A. Montgomery, K. Raghavachari, M. A. Al-Laham, V. G. Zakrzewski, J. V. Ortiz, J. B. Foresman, J. Cioslowski, B. B. Stefanov, A. Nanayakkara, M. Challacombe, C. Y. Peng, P. Y. Ayala, W. Chen, M. W. Wong, J. L. Andres, E. S. Replogle, R. Gomperts, R. L. Martin, D. J. Fox, J. S. Binkley, D. J.

DeFrees, J. Baker, J. P. Stewart, M. Head-Gordon, C. Gonzalez, and J. A. Pople, GAUSSIAN 94, Gaussian, Inc., Pittsburgh PA, 1995.
[45] MOLPRO is a package of *ab initio* programs written by H.-J. Werner and P. J. Knowles, with contributions by J. Almlöf, R. D. Amos, M. J. O. Deegan, S. T. Elbert, C. Hampel, W. Meyer, K. Peterson, R. M. Pitzer, A. J. Stone, P. R. Taylor, and R. Lindh.
[46] P. C. Hariharan and J. A. Pople, Theor. Chim. Acta **28**, 213 (1973).
[47] R. Krishnan, J. S. Binkley, R. Seeger, and J. A. Pople, J. Chem. Phys. **72**, 650 (1980).
[48] T. Clark, J. Chandrasekhar, G. W. Spitznagel, and P. v. R. Schleyer, J. Comput. Chem. **4**, 294 (1983).
[49] M. J. Frisch, J. A. Pople, and J. S. Binkley, J. Chem. Phys. **80**, 3265 (1984).
[50] T. H. Dunning, Jr., J. Chem. Phys. **90**, 1007 (1989).
[51] R. A. Kendall, T. H. Dunning, Jr., and R. J. Harrison, J. Chem. Phys. **96**, 6796 (1992).
[52] C. Møller and M. S. Plesset, Phys. Rev. **46**, 618 (1934).
[53] J. A. Pople, J. S. Binkley, and R. Seeger, Int. J. Quantum Chem. Symp. **10**, 1 (1976).
[54] R. Krishnan and J. A. Pople, Int. J. Quantum Chem. **14**, 91 (1978).
[55] R. Krishnan, M. J. Frisch, and J. A. Pople, J. Chem. Phys. **72**, 4244 (1980).
[56] J. A. Pople, M. Head-Gordon, and K. Raghavachari, J. Chem. Phys. **87**, 5968 (1987).
[57] K. Raghavachari, G. W. Trucks, J. A. Pople, and M. Head-Gordon, Chem. Phys. Lett. **157**, 479 (1989).
[58] M. J. O. Deegan and P. J. Knowles, Chem. Phys. Lett. **227**, 321 (1994).
[59] R. J. Bartlett, J. Phys. Chem. **93**, 1697 (1989).
[60] C. Hampel, K. Peterson, and H.-J. Werner, Chem. Phys. Lett. **190**, 1 (1992).
[61] A. L. L. East, C. S. Johnson, and W. D. Allen, J. Chem. Phys. **98**, 1299 (1993).
[62] R. J. Bartlett and I. Shavitt, Chem. Phys. Lett. **50**, 190 (1977).
[63] W. D. Laidig, G. Fitzgerald, and R. J. Bartlett, Chem. Phys. Lett. **113**, 151 (1985).
[64] N. C. Handy, P. J. Knowles, and K. Somasundram, Theor. Chim. Acta **68**, 87 (1985).
[65] N. C. Handy, R. D. Amos, J. F. Gaw, J. E. Rice, and E. D. Simandiras, Chem. Phys. Lett. **120**, 151 (1985).
[66] E. D. Simandiras, N. C. Handy, and R. D. Amos, Chem. Phys. Lett. **133**, 324 (1987).
[67] W. D. Allen, A. G. Császár, and D. A. Horner, J. Am. Chem. Soc. **114**, 6834 (1992).
[68] P. Pulay and F. Török, Acta Chim. Acad. Sci. Hung. **44**, 287 (1965).
[69] G. Keresztury and G. Jalsovszky, J. Mol. Struct. **10**, 304 (1971).
[70] J. Overend, in *Infrared Spectroscopy and Molecular Structure*, edited by M. Davies (Elsevier, Amsterdam, 1963), p. 345.
[71] G. Zerbi, in *Vibrational Intensities in Infrared and Raman Spectroscopy*, edited by W. B. Person and G. Zerbi (Elsevier, Amsterdam, 1982).
[72] W. D. Allen, INTDER94, Stanford, 1994 version. INTDER is a set of codes for performing general curvilinear transformations of coordinates and force constants, as well as harmonic frequency analyses.
[73] G. Aissing and H. J. Monkhorst, Int. J. Quantum Chem. **43**, 733 (1992).
[74] A. L. L. East and L. Radom, J. Mol. Struct. **376**, 437 (1996).
[75] W. D. Allen, A. L. L. East, and A. G. Császár, in *Structures and Conformations of Non-Rigid Molecules*, edited by J. Lanne, M. Dakkouri, B. van der Veken, and H. Oberhammer (Kluwer, Dordrecht, 1993), p. 343.
[76] W. D. Allen, private communication.
[77] A. P. Scott, A. L. L. East, and L. Radom, work in progress.
[78] A. L. L. East, W. D. Allen, and S. J. Klippenstein, J. Chem. Phys. **102**, 8506 (1995).
[79] R. D. Brown, R. F. C. Brown, F. W. Eastwood, P. D. Godfrey, and D. McNaughton, J. Am. Chem. Soc. **101**, 4705 (1979).
[80] S. Ekern, J. Szczepanski, and M. Vala, J. Phys. Chem. **100**, 16,109 (1996).